

CircRNF20 aggravates the progression of non-small-cell lung carcinoma by activating MAPK9

Z.-X. WANG¹, Y. ZHAO², Y.-B. WANG³, Q. ZHANG⁴, Q.-X. ZOU¹,
F.-H. LIANG⁵, F.-W. LIN¹

¹Department of Thoracic Surgery, China-Japan Union Hospital of Jilin University, Changchun, China

²Medical Examination Center, The Second Hospital of Jilin University, Changchun, China

³Second Department of Orthopaedics, Meihekou Central Hospital, Meihekou, China

⁴Department of Thoracic Surgery, Jilin Province People's Hospital, Changchun, China

⁵Cardiovascular Thoracic Surgery, The Second Affiliated Hospital of Guangxi Medical University, Nanning, China

Abstract. – OBJECTIVE: To explore the clinical significance of circRNF20 in non-small-cell lung carcinoma (NSCLC), and its regulatory effects on NSCLC cell functions by activating MAPK9.

PATIENTS AND METHODS: Relative levels of circRNF20 and MAPK9 in NSCLC tissues were detected by quantitative Real Time-Polymerase Chain Reaction (qRT-PCR). The relationship between circRNF20, MAPK9 and pathological factors in NSCLC patients was analyzed. Prognostic potentials of circRNF20 and MAPK9 in NSCLC were assessed by Kaplan-Meier method. The interaction between circRNF20 and MAPK9 was tested by Dual-Luciferase reporter assay. Regulatory effects of circRNF20 and MAPK9 on proliferative abilities in H358 and SPC-A1 cells were examined by Cell Counting Kit-8 (CKK-8) and colony formation assay.

RESULTS: CircRNF20 and MAPK9 were upregulated in NSCLC tissues than normal ones. They were correlated to T stage and poor prognosis in NSCLC patients, while their levels were unrelated to gender, age, and incidences of lymphatic and distant metastasis. Knockdown of circRNF20 attenuated proliferative abilities in H358 and SPC-A1 cells. On the contrary, the overexpression of MAPK9 yielded the opposite results. MAPK9 was the target gene binding circRNF20, which was able to reverse the regulatory effect of circRNF20 on NSCLC proliferation.

CONCLUSIONS: CircRNF20 and MAPK9 are upregulated in NSCLC cases, which are closely linked to T stage in NSCLC patients. They are independent prognostic factors for NSCLC. By activating MAPK9, circRNF20 stimulates NSCLC proliferation.

Key Words:

CircRNF20, MAPK9, NSCLC, Proliferation.

Introduction

Although the diagnostic and therapeutic strategies of lung cancer have been improved, the 5-year survival of lung cancer is lower than 15%, which severely threatens human health¹. The mortality and morbidity of lung cancer are in the first place of all malignant tumors globally¹⁻³. Lung cancer is histologically classified to non-small-cell lung carcinoma (NSCLC) and small-cell lung carcinoma (SCLC). The vast majority (85%) of lung cancer cases are NSCLC, including adenocarcinoma and squamous cell carcinoma^{4,5}. NSCLC is highly malignant, and the hematogenous and lymphatic metastases can be detected in the early phase of NSCLC, leading to a poor prognosis¹⁻⁶. Currently, surgical resection is preferred to early stage NSCLC. Nevertheless, a large number of people are diagnosed as advanced stage NSCLC because effective and specific diagnostic biomarkers are lacked, and these patients are unable to be operated^{7,8}. These patients can be benefited from chemotherapy and radiotherapy. However, primary or secondary drug resistance is an obstacle in anti-cancer treatment^{8,9}. The pathogenesis of NSCLC is very complicated, which remains largely unknown^{10,11}. Gene mutations and abnormalities in tumor-associated pathways are risk factors for carcinogenesis of NSCLC^{12,13}.

In human genomes, only 2% of them are protein-encoding genes, and the majority are non-coding RNAs¹⁴. MiRNAs and lncRNAs are involved in human diseases by regulating gene transcription and translation^{14,15}. As a novel type of noncoding RNAs, the biological functions of circRNAs are required to be further explored¹⁶.

They are used to be considered as by-products of precursor RNA splicing. It is indicated that non-coding RNAs are diverse and eukaryotic transcriptome is complex^{16,17}. Unlike traditional linear RNAs, circRNAs lack the 5' or 3' end because of the covalent closed structure¹⁸. Featured by high abundances, high conservatism and specific expressions, circRNAs are considered as potential cancer biomarkers¹⁷⁻²⁰. This study aims to explore the clinical significance of circRNF20 in NSCLC and the underlying mechanism.

Patients and Methods

NSCLC Patients and Tissue Samples

Cancer and normal tissues were collected from 44 NSCLC patients after informed consent. All samples were harvested from surgery, puncture biopsy or bronchoscopy biopsy. None of them had anti-cancer treatment before surgery. Tumor node metastasis (TNM) staging of NSCLC was determined based on the criteria proposed by The Union for International Cancer Control (UICC). Inclusion criteria: patients with no severe diseases in other organs and those undergoing no preoperative chemotherapy and post-operative radiotherapy. Exclusion criteria: patients with distant metastasis, those complicated with other malignancies, those with mental disease, those complicated with myocardial infarction, heart failure or those previously exposed to radioactive rays. All patients were followed up after discharge by telephone or outpatient review, including baseline characteristics, clinical symptoms and imaging examination. This investigation was approved by the Ethics Committee of China-Japan Union Hospital of Jilin University. Signed written informed consents were obtained from all participants before the study.

Cell Lines and Reagents

NSCLC cell lines (A549, H1299, H358, SPC-A1) and the pulmonary epithelial cell line (BEAS-2B) were purchased from Cell Bank of Type Culture Collection. They were cultivated in Dulbecco's Modified Eagle's Medium (DMEM; Thermo Fisher Scientific, Waltham, MA, USA) with 10% fetal bovine serum (FBS; Gibco, Rockville, MD, USA) in a 5% CO₂ incubator at 37°C.

Transfection

CircRNF20 shRNA, pcDNA3.1-MAPK9 and negative controls were synthesized by GenePharma (Shanghai, China). Cells in 6-well plates were

cultured to 40-60% confluence and transfected using Lipofectamine 2000 (Invitrogen, Carlsbad, CA, USA). They were collected for use after 48 h.

Cell Proliferation Assay

5×10³ cells were implanted in each well of a 6-well plate, where 10 μL of Cell Counting Kit-8 (CCK-8) solution was added (TaKaRa, Dalian, China). After 1-h culturing in the dark, 450 nm absorbance was measured using a microplate reader. Blank group was set by adding medium and experimental solution without cells.

Colony Formation Assay

Cells were inoculated in a 6-well plate with 100 cells per well and cultured for 2 weeks. Culture medium was replaced once in the first week and twice in the second week. Visible colonies were washed in phosphate-buffered saline (PBS), fixed in methanol for 20 min and dyed in 0.1% crystal violet for 20 min, which were finally captured and calculated.

Quantitative Real-Time Polymerase Chain Reaction (qRT-PCR)

TRIzol reagent (Invitrogen, Carlsbad, CA, USA) was used for isolating total cellular RNAs, followed by incubation with chloroform. After 10-min centrifugation at 4°C, the upper layer was collected and incubated with 700 μL of isopropanol. The mixture was centrifuged at 4°C, 12,000 rpm for 10 min. The precipitant was washed in 75% ethanol and air dried. The collected RNAs were reversely transcribed into complementary deoxyribose nucleic acids (cDNAs; PrimeScript RT Reagent; TaKaRa, Otsu, Shiga, Japan). Using the SYBR[®] Premix Ex Taq[™] kit (TaKaRa, Otsu, Shiga, Japan), StepOne Plus Real-time PCR system (Applied Biosystems, Foster City, CA, USA), and qRT-PCR was carried out. Relative level was calculated by 2^{-ΔΔC_t} and normalized to that of glyceraldehyde 3-phosphate dehydrogenase (GAPDH). circRNF20: forward: 5'-GAGCCGTGTCCCAGATTGT-3', reverse: 5'-TGCCGCTGATCCAACATTTC-3'; MAPK9: forward: 5'-ACCCTTCGGGATATTGCAGG-3', reverse: 5'-TGCAGCACAAACAATCCCTTG-3'; GAPDH: forward: 5'-TGTGGGCATCAATGATTGG-3', reverse: 5'-ACACCATGTATTCGGGTCAAT-3'.

Western Blot

Cells were lysed in radioimmunoprecipitation assay (RIPA) buffer (Beyotime, Shanghai, China) on ice for 30 min. Cell lysate was centrifuged at 4°C, 14000×g for 15 min. Extracted protein sam-

ples were quantified by bicinchoninic acid (BCA) method (Pierce, Rockford, IL, USA). Protein samples were electrophoresed in 10% Sodium Dodecyl Sulfate Polyacrylamide Gel Electrophoresis (SDS-PAGE), and loaded on polyvinylidene difluoride (PVDF) membranes (Millipore, Billerica, MA, USA). Next, non-specific antigens were blocked in 5% skim milk for 2 hours. Membranes were reacted with primary and secondary antibodies for indicated time. Band exposure and analyses of grey values were finally conducted.

Dual-Luciferase Reporter Assay

Wild-type and mutant-type circRNF20 vectors were constructed based on the predicted consequential pairing of the seed sequence in the 3'-untranslated region (3'-UTR) of circRNF20 and MAPK9. CircRNF20-WT and circRNF20-MUT were co-transfected into cells with pcDNA3.1-NC or pcDNA3.1-MAPK9, respectively. After 48 h co-transfection, Luciferase activity was measured (Promega, Madison, WI, USA).

Statistical Analysis

Data were expressed as mean \pm standard deviation and analyzed by Statistical Product and Service Solutions (SPSS) 20.0 (SPSS IBM Corp., Armonk, NY USA). Differences between groups were analyzed by the *t*-test. The relationship between circRNF20, MAPK9 and pathological factors in NSCLC patients was assessed by Chi-square test. Overall survival was assessed by Kaplan-Meier method and log-rank test. A significant difference was set at $p < 0.05$.

Results

Expression Pattern of CircRNF20 in NSCLC

We collected 44 cases of NSCLC tissues and normal ones for detecting circRNF20 levels. It is shown that circRNF20 was upregulated in 40/44 NSCLC tissues, and weekly positive or negative expression of circRNF20 was only detected in 4/44 cancer tissues (Figure 1A). Baseline characteristics of recruited NSCLC patients were

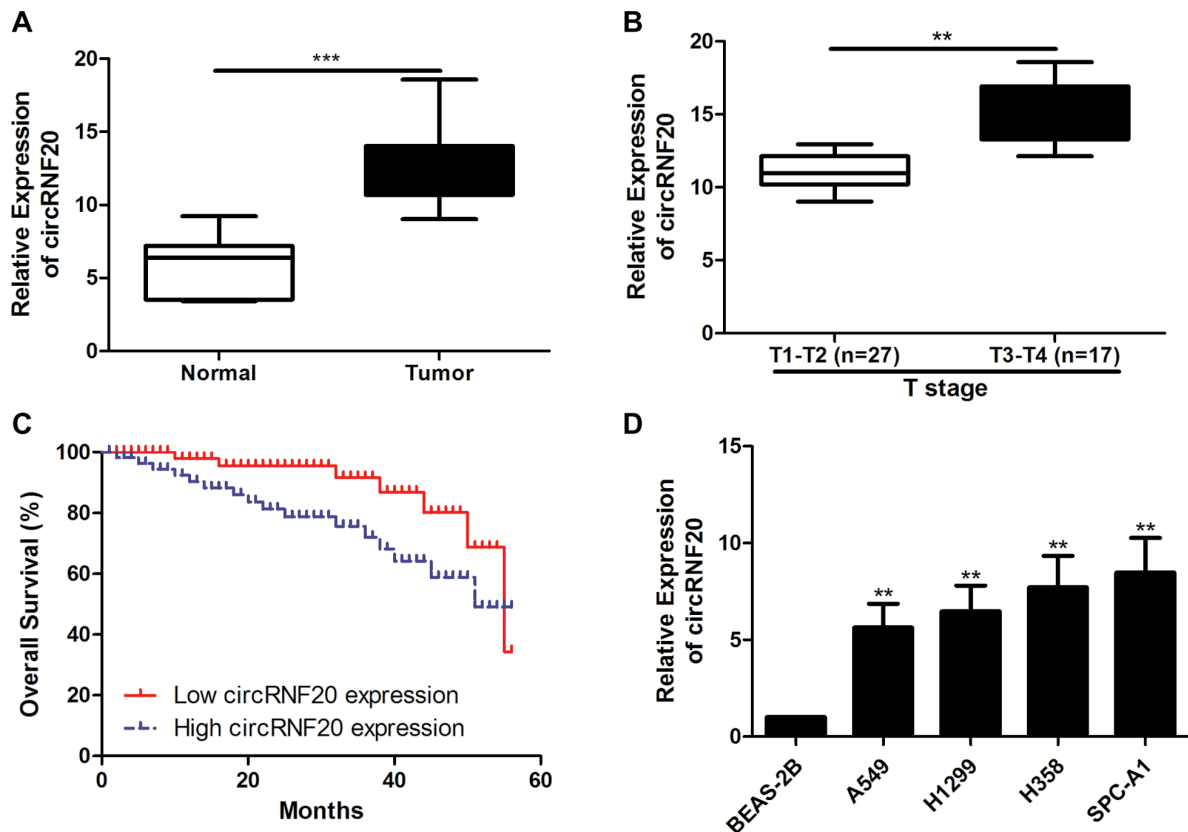


Figure 1. Expression pattern of circRNF20 in NSCLC. **A**, Relative levels of circRNF20 in NSCLC tissues and normal ones. **B**, Relative levels of circRNF20 in T1-T2 (n=27) and T3-T4 (n=17) NSCLC tissues. **C**, Overall survival in NSCLC patients expressing high or low level of circRNF20. **D**, Relative levels of circRNF20 in NSCLC cell lines. Data were expressed as mean \pm SD; * $p < 0.05$, ** $p < 0.01$, *** $p < 0.001$.

Table I. Association of circRNF20 and MAPK9 expression with clinicopathologic characteristics of non-small cell lung cancer.

Parameters	No. of cases	circRNF20 expression		p-value	MAPK9 expression		p-value
		Low (%)	High (%)		Low (%)	High (%)	
Age (years)				0.387			0.977
<60	18	10	8		7	11	
≥60	26	11	15		10	16	
Gender				0.537			0.944
Male	22	12	11		9	14	
Female	22	9	12		8	13	
T stage				0.023			0.004
T1-T2	27	17	11		15	12	
T3-T4	17	4	12		2	15	
Lymph node metastasis				0.169			0.431
No	28	16	13		10	19	
Yes	16	5	10		7	8	
Distance metastasis				0.305			0.242
No	27	15	13		9	19	
Yes	17	6	10		8	8	

analyzed. As shown in Table I, circRNF20 was correlated to T stage in NSCLC patients, while unrelated to gender, age and incidences of lymphatic and distant metastasis. qRT-PCR results consistently revealed higher level of circRNA20 in T3-T4 NSCLC patients compared with T1-T2 patients (Figure 1B). Kaplan-Meier curves were depicted for assessing the prognostic potential of circRNF20 in NSCLC. High level of circRNF20 predicted poor prognosis in NSCLC patients (Figure 1C). Subsequently, circRNF20 levels in NSCLC cell lines were detected. Compared with the pulmonary epithelial cell line, circRNF20 was upregulated in NSCLC cell lines (Figure 1D).

Knockdown of CircRNF20 Weakened Proliferative Ability in NSCLC

H358 and SPC-A1 cells were used for constructing circRNF20 knockdown models. They were transfected with sh-NC or sh-circRNF20, followed by puromycin screen (Figure 2A). Knockdown of circRNF20 markedly decreased cell viability and colony number in H358 and SPC-A1 cells, suggesting the inhibited proliferative ability (Figure 2B, 2C).

Expression Pattern of MAPK9 in NSCLC

Bioinformatics analysis indicated the binding between circRNF20 and MAPK9. We subsequently detected MAPK9 levels in NSCLC cases. Compared with normal tissues, MAPK9 was upregulated in NSCLC tissues, especially T3-T4 cases (Figure 3A, 3B). By analyzing clinical data of NSCLC patients, it is found that MAPK9 was

correlated to T stage in NSCLC patients, rather than the other factors (Table I). In addition, NSCLC patients expressing high level of MAPK9 had worse overall survival than those expressing low level (Figure 3C). CircRNF20 level was positively correlated to that of MAPK9 in NSCLC tissues (Figure 3D).

Overexpression of MAPK9 Facilitated Proliferative Ability in NSCLC

We next explored the involvement of MAPK9 in regulating NSCLC cell functions. Transfection of pcDNA3.1-MAPK9 effectively upregulated MAPK9 in H358 and SPC-A1 cells (Figure 4A). In NSCLC cells overexpressing MAPK9, cell viability and colony number markedly increased than those of controls (Figure 4B, 4C).

CircRNF20 Regulated NSCLC Proliferation by Activating MAPK9

Based on the predicted binding sites in the 3'-UTR of MAPK9 and circRNF20, wild-type and mutant-type circRNF20 vectors were constructed. Dual-Luciferase reporter assay confirmed the binding between MAPK9 and circRNF20 (Figure 5A). Co-transfection of sh-circRNF20 downregulated protein level of MAPK9 in H358 and SPC-A1 cells overexpressing MAPK9 (Figure 5B). Compared with NSCLC cells co-transfected with sh-NC and pcDNA3.1-MAPK9, viability and colony number were lower in cells co-transfected with sh-circRNF20 and pcDNA3.1-MAPK9 (Figure 5C, 5D). It is indicated that circRNF20 and MAPK9 synergistically regulated NSCLC proliferation.

Discussion

Globally, cancer is the second leading cause of deaths following cardiac diseases. The incidence and mortality of lung cancer are on the rise, and

they rank the top place in male cancers¹⁻³. In recent years, the number of cancer patients in our country has largely increased. There are more than 4.29 million new cancer cases each year in China, accounting for 20% of global cases. Severely, 2.81

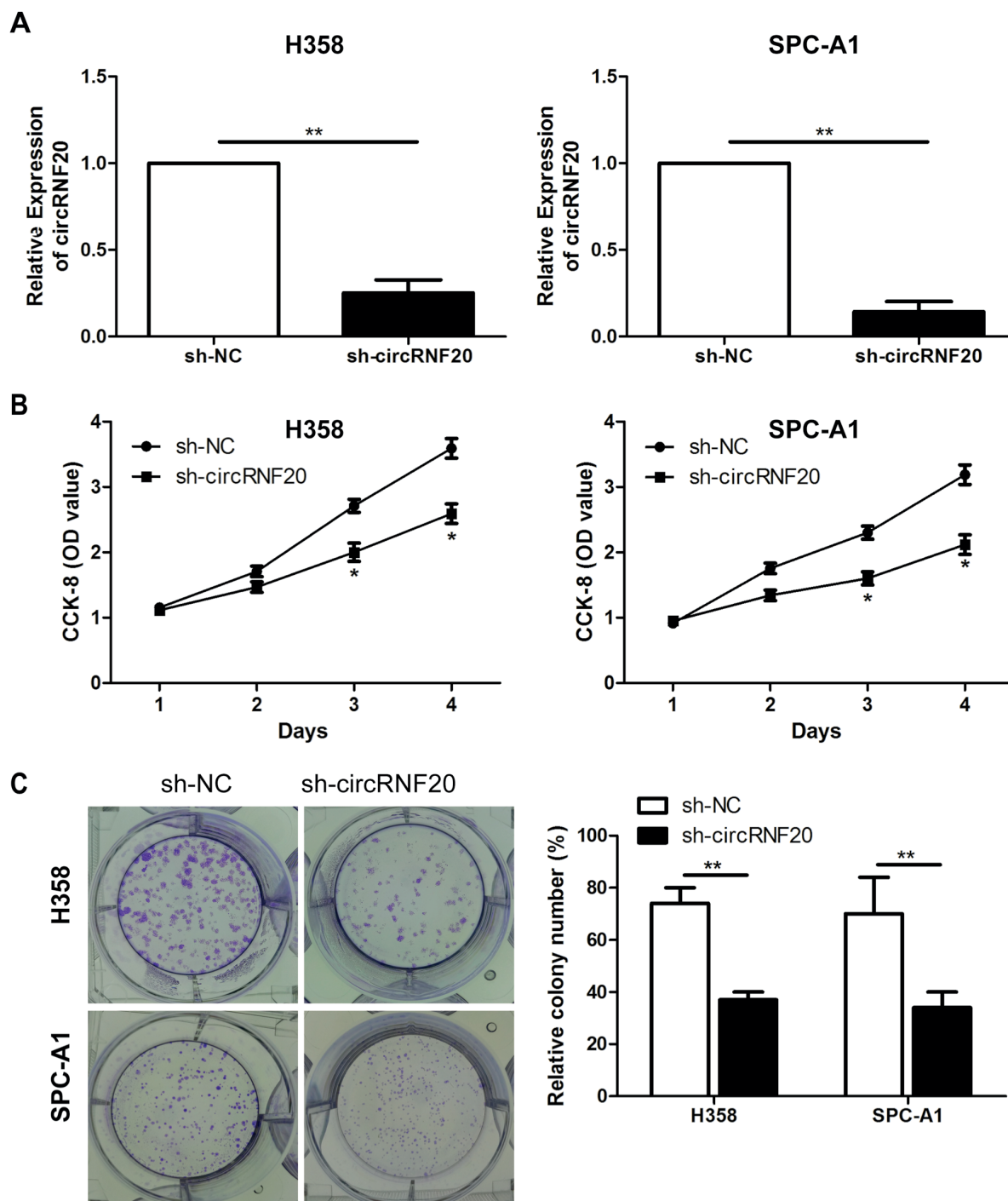


Figure 2. Knockdown of circRNF20 weakened proliferative ability in NSCLC. **A**, Transfection efficacy of sh-circRNF20 in H358 and SPC-A1 cells. **B**, Viability in H358 and SPC-A1 cells transfected with sh-NC or sh-circRNF20. **C**, Colony number in H358 and SPC-A1 cells transfected with sh-NC or sh-circRNF20 (magnification 10×). Data were expressed as mean±SD; * $p < 0.05$, ** $p < 0.01$.

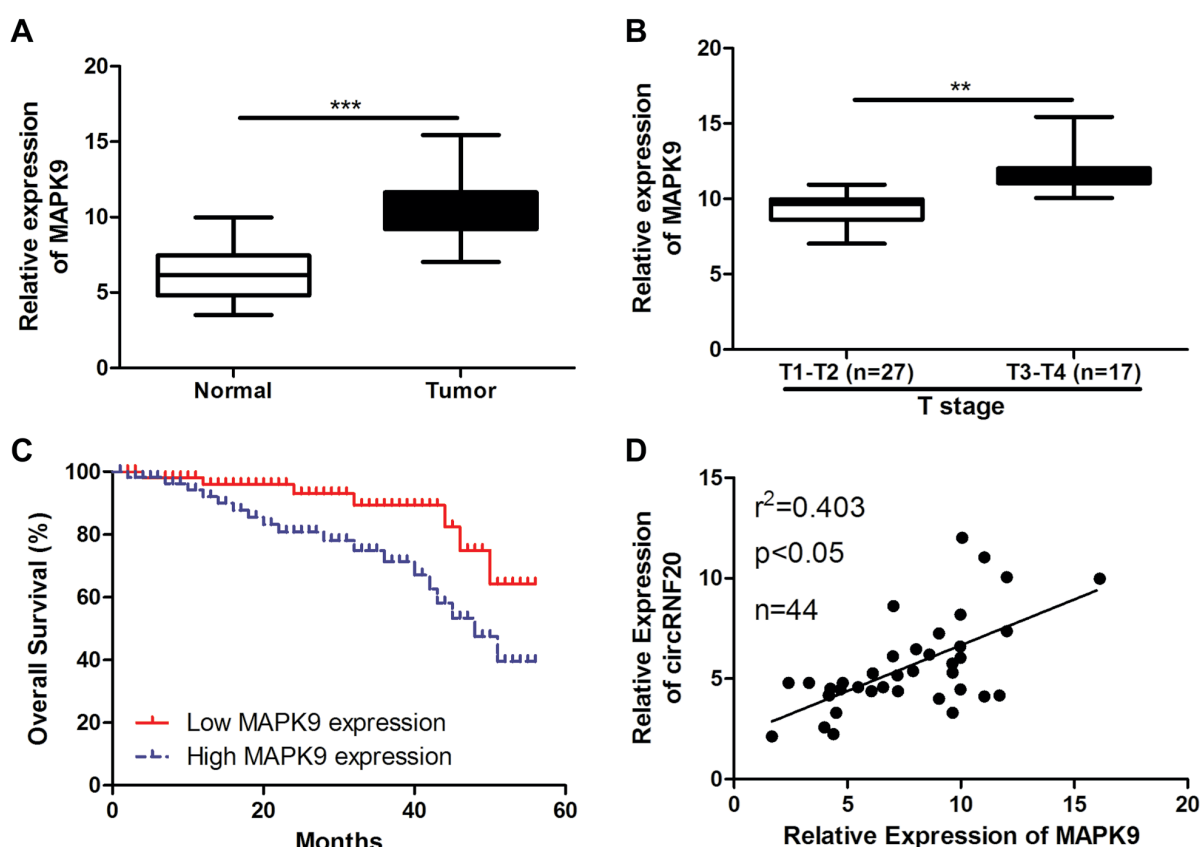


Figure 3. Expression pattern of MAPK9 in NSCLC. **A**, Relative levels of MAPK9 in NSCLC tissues and normal ones. **B**, Relative levels of MAPK9 in T1-T2 (n=27) and T3-T4 (n=17) NSCLC tissues. **C**, Overall survival in NSCLC patients expressing high or low level of MAPK9. **D**, Correlation between relative levels of circRNF20 and MAPK9 in NSCLC tissues. Data were expressed as mean±SD; ** $p < 0.01$, *** $p < 0.001$.

million people die of cancers annually in our country^{2,4}. At present, lung cancer is one of the largest threats to human health and even lives³⁻⁵. It is urgent to clarify the pathogenesis of lung cancer, and to improve therapeutic efficacy⁸⁻¹².

The complicated relationship between circRNAs and cancers^{17,19,20} concern also the role of circRNAs in regulating biological functions *via* exerting the effect of miRNA sponge. As a result, circRNAs may be promising cancer biomarkers to be utilized in clinical application. Previous studies^{11,12} have proposed novel molecular biomarkers for NSCLC, which are beneficial to individualized therapy and prognosis assessment. Cao et al²¹ suggested that circRNF20 promoted the progression of breast cancer. However, the potential influences of circRNF20 on NSCLC progression remain largely unclear. In this study, 44 cases of NSCLC tissues and normal ones were collected to detect differential expressions of circRNF20. The data uncovered that circRNF20 was

upregulated in NSCLC tissues. Moreover, it was related to T stage and poor prognosis in NSCLC patients. Subsequently, circRNF20 knockdown model was constructed by transfection of sh-circRNF20 in H358 and SPC-A1 cells. Knockdown of circRNF20 remarkably decreased viability and colony number in NSCLC cells, suggesting the inhibited proliferative ability of NSCLC.

Using the bioinformatics tool, we discovered the potential binding sites in the 3'-UTR of circRNF20 and MAPK9. Similar to the expression pattern and clinical significance of circRNF20, MAPK9 was upregulated in NSCLC tissues, and it was correlated T stage and overall survival of NSCLC patients. A positive correlation between the levels of circRNF20 and MAPK9 was identified in NSCLC tissues. Overexpression of MAPK9 remarkably promoted the proliferative ability in NSCLC cells. According to the predicted binding sites, Luciferase vectors targeting circRNF20 were constructed. The overexpression of

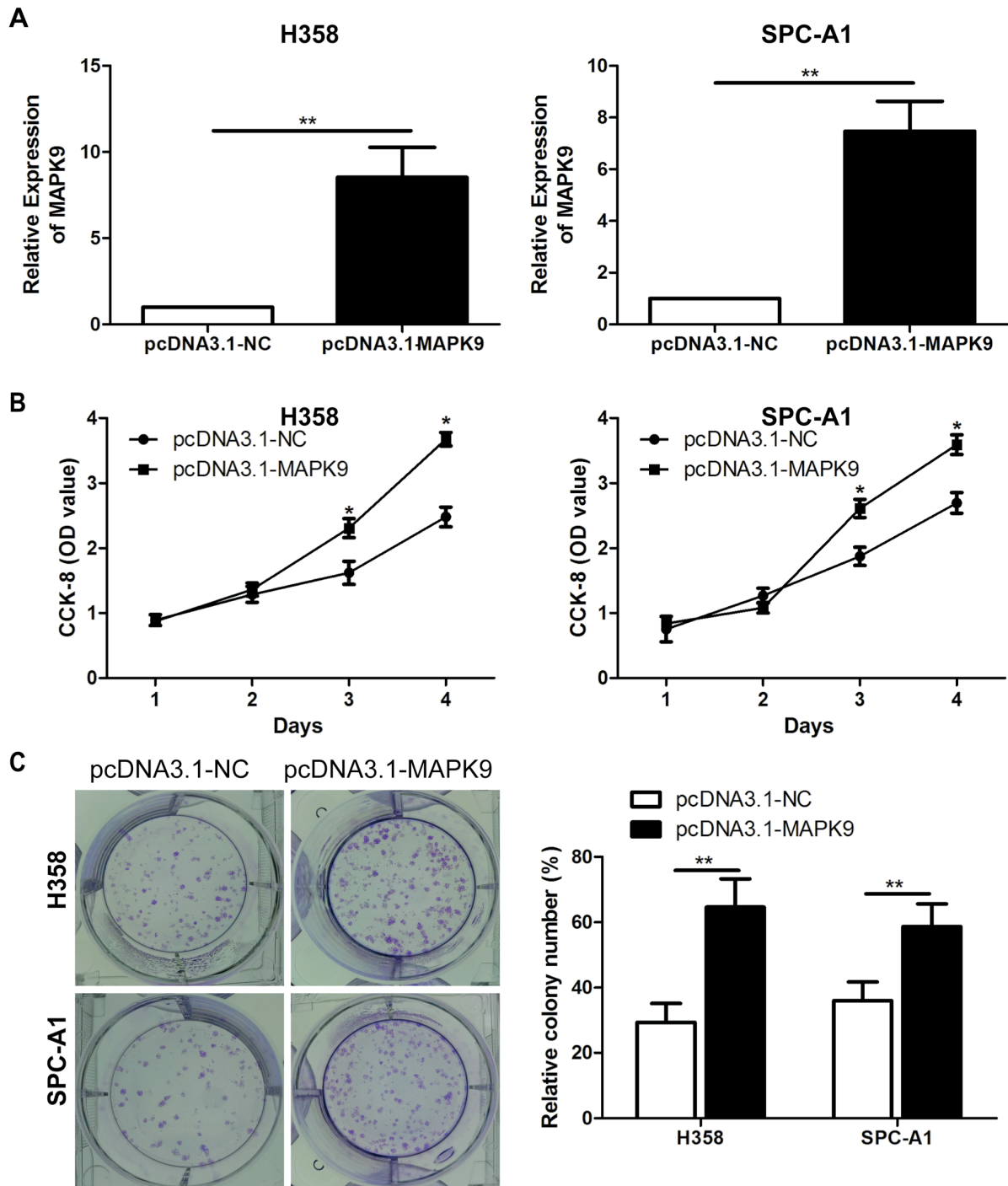


Figure 4. Overexpression of MAPK9 facilitated proliferative ability in NSCLC. **A**, Transfection efficacy of pcDNA3.1-MAPK9 in H358 and SPC-A1 cells. **B**, Viability in H358 and SPC-A1 cells transfected with pcDNA3.1-NC or pcDNA3.1-MAPK9. **C**, Colony number in H358 and SPC-A1 cells transfected with pcDNA3.1-NC or pcDNA3.1-MAPK9 (magnification 10×). Data were expressed as mean±SD; * $p < 0.05$, ** $p < 0.01$.

MAPK9 could decrease the Luciferase activity in the wild-type circRNF20 vector, while it did not influence Luciferase activity in the mutant-type

one, confirming the binding between MAPK9 and circRNF20. We thereafter speculated the involvement of MAPK9 regulated by circRNF20

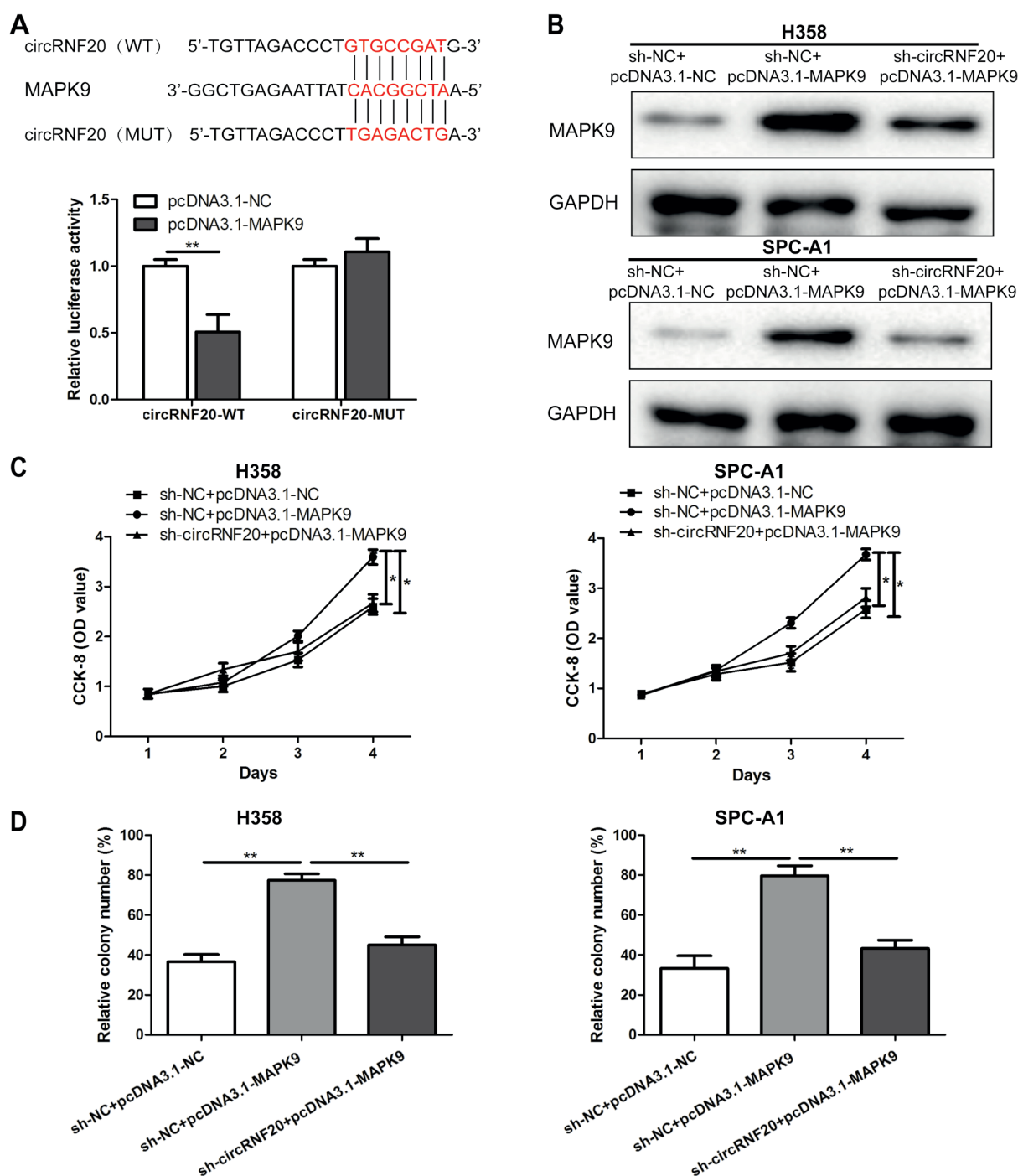


Figure 5. CircRNF20 regulated NSCLC proliferation by activating MAPK9. **A**, Dual-Luciferase reporter assay showed the binding between circRNF20 and MAPK9. **B**, Protein level of MAPK9 in H358 and SPC-A1 cells co-transfected with sh-NC+pcDNA3.1-NC, sh-NC+pcDNA3.1-MAPK9 or sh-circRNF20+pcDNA3.1-MAPK9. **C**, Viability in H358 and SPC-A1 cells co-transfected with sh-NC+pcDNA3.1-NC, sh-NC+pcDNA3.1-MAPK9 or sh-circRNF20+pcDNA3.1-MAPK9. **D**, Colony number in H358 and SPC-A1 cells co-transfected with sh-NC+pcDNA3.1-NC, sh-NC+pcDNA3.1-MAPK9 or sh-circRNF20+pcDNA3.1-MAPK9; Data were expressed as mean±SD; * $p < 0.05$, ** $p < 0.01$.

in the progression of NSCLC. Interestingly, the overexpression of MAPK9 could abolish the regulatory effect of circRNF20 on the proliferation

ability of NSCLC. To sum up, as a novel oncogenic gene, circRNF20 aggravated the malignant progression of NSCLC by activating MAPK9,

which became a promising biomarker for diagnosis and treatment for NSCLC.

Conclusions

In summary, circRNF20 and MAPK9 are up-regulated in NSCLC cases, which are closely linked to T stage in NSCLC patients. They are independent prognostic factors for NSCLC. By activating MAPK9, circRNF20 stimulates NSCLC proliferation.

Conflict of Interest

The Authors declare that they have no conflict of interests.

References

- PURI S, SALTOS A, PEREZ B, LE X, GRAY JE. Locally advanced, unresectable non-small cell lung cancer. *Curr Oncol Rep* 2020; 22: 31.
- BADE BC, DELA CC. Lung Cancer 2020: epidemiology, etiology, and prevention. *Clin Chest Med* 2020; 41: 1-24.
- USMAN AM, MILLER J, PEIRSON L, FITZPATRICK-LEWIS D, KENNY M, SHERIFALI D, RAINA P. Screening for lung cancer: a systematic review and meta-analysis. *Prev Med* 2016; 89: 301-314.
- SAAB S, ZALZALE H, RAHAL Z, KHALIFEH Y, SINJAB A, KADARA H. Insights into lung cancer immune-based biology, prevention, and treatment. *Front Immunol* 2020; 11: 159.
- TRAVIS WD. Lung cancer pathology: current concepts. *Clin Chest Med* 2020; 41: 67-85.
- QIANG H, CHANG Q, XU J, QIAN J, ZHANG Y, LEI Y, HAN B, CHU T. New advances in antiangiogenic combination therapeutic strategies for advanced non-small cell lung cancer. *J Cancer Res Clin Oncol* 2020; 146: 631-645.
- HERBST RS, MORGENZSTERN D, BOSHOFF C. The biology and management of non-small cell lung cancer. *Nature* 2018; 553: 446-454.
- MALIK N, PALMA D. Oligometastatic non-small cell lung cancer: where do we go next? *Lung Cancer* 2017; 106: 145-147.
- PASSIGLIA F, BERTOLACCINI L, DEL RM, FACCHINETTI F, FERRARA R, FRANCHINA T, MALAPELLE U, MENIS J, PASSARO A, PILOTTO S, RAMELLA S, ROSSI G, TRISOLINI R, NOVELLO S. Diagnosis and treatment of early and locally advanced non-small-cell lung cancer: The 2019 AIOM (Italian Association of Medical Oncology) clinical practice guidelines. *Crit Rev Oncol Hematol* 2020; 148: 102862.
- GIULIANI ME, ROBINSON CG, SALAMA JK, DALY ME. Oligoreview of non-small cell lung cancer oligometastases. *Int J Radiat Oncol Biol Phys* 2020; 106: 455-459.
- CHENG H, PEREZ-SOLER R. Leptomeningeal metastases in non-small-cell lung cancer. *Lancet Oncol* 2018; 19: e43-e55.
- VAN DEN BROEK D, HILTERMANN T, BIESMA B, DINJENS W, T HN, HINRICHS J, LEERS M, MONKHORST K, VAN OOSTERHOUT M, SCHARNHORST V, SCHUURING E, SPEEL EM, VAN DEN HEUVEL MM, VAN SCHAIK R, VON DER THUSEN J, WILLEMS SM, DE VISSER L, LIGTENBERG M. Implementation of novel molecular biomarkers for non-small cell lung cancer in the Netherlands: how to deal with increasing complexity. *Front Oncol* 2019; 9: 1521.
- RIJAVEC E, COCO S, GENOVA C, ROSSI G, LONGO L, GROSSI F. Liquid biopsy in non-small cell lung cancer: highlights and challenges. *Cancers (Basel)* 2019; 12: 17.
- SEAL RL, CHEN LL, GRIFFITHS-JONES S, LOWE TM, MATHEWS MB, O'REILLY D, PIERCE AJ, STADLER PF, ULITSKY I, WOLIN SL, BRUFORD EA. A guide to naming human non-coding RNA genes. *EMBO J* 2020; 39: e103777.
- KAZIMIERCZYK M, KASPROWICZ MK, KASPRZYK ME, WRZESINSKI J. Human long noncoding RNA interactome: detection, characterization and function. *Int J Mol Sci* 2020; 21: 1027.
- CHEN LL, YANG L. Regulation of circRNA biogenesis. *RNA Biol* 2015; 12: 381-388.
- ZHANG HD, JIANG LH, SUN DW, HOU JC, JI ZL. CircRNA: a novel type of biomarker for cancer. *Breast Cancer* 2018; 25: 1-7.
- DU WW, ZHANG C, YANG W, YONG T, AWAN FM, YANG BB. Identifying and characterizing circRNA-protein interaction. *Theranostics* 2017; 7: 4183-4191.
- MENG S, ZHOU H, FENG Z, XU Z, TANG Y, LI P, WU M. CircRNA: functions and properties of a novel potential biomarker for cancer. *Mol Cancer* 2017; 16: 94.
- KRISTENSEN LS, HANSEN TB, VENO MT, KJEMS J. Circular RNAs in cancer: opportunities and challenges in the field. *Oncogene* 2018; 37: 555-565.
- CAO L, WANG M, DONG Y, XU B, CHEN J, DING Y, QIU S, LI L, KARAFILOVA ZE, ZHOU X, XU Y. Circular RNA circRNF20 promotes breast cancer tumorigenesis and Warburg effect through miR-487a/HIF-1alpha/HK2. *Cell Death Dis* 2020; 11: 145.